AIP | The Journal of Chemical Physics

Molecular alignment using coherent resonant excitation: A new proposal for stereodynamic control of chemical reactions

Nandini Mukherjee

Citation: J. Chem. Phys. **131**, 164302 (2009); doi: 10.1063/1.3249970
View online: http://dx.doi.org/10.1063/1.3249970
View Table of Contents: http://jcp.aip.org/resource/1/JCPSA6/v131/i16
Published by the American Institute of Physics.

Molecular alignment using coherent resonant excitation: A new proposal for stereodynamic control of chemical reactions

Nandini Mukherjee[a)]
Department of Physics and Astronomy, University of California, Los Angeles, California 90095, USA

(Received 26 July 2009; accepted 28 September 2009; published online 26 October 2009)

For the mode-selective control of chemical reaction, we present a new approach of molecular alignment using coherent resonant interaction with low intensity midinfrared optical pulses. Under coherent excitation, the alignment of vibrationally excited molecules becomes a function of the optical pulse area. Depending on the type of transition, with certain values of the pulse areas, a narrow group of magnetic substates are selectively excited, which results in aligning the rotational axis of the molecular ensemble. It is shown that for a *P*-type transition, significant alignment in the excited vibrational state can be realized using a resonant midinfrared pulse of area $\approx 2\pi$. Under the steady state excitation (pulse duration longer than the vibrational relaxation time), the molecular alignment is destroyed due to saturation. We design a polarization spectroscopy experiment to coherently excite and probe the molecular alignment in real time. © *2009 American Institute of Physics*. [doi:10.1063/1.3249970]

I. INTRODUCTION

The mode-selective control of chemical reactions requires excitation of molecules into preselected rotational vibrational levels. Pioneering experiments of Kary and Zare[1] and other researchers[2,3] have shown that vibrational excitation of reagent molecules enhances the rate of a chemical reaction by many orders of magnitudes. Lui *et al.*[3] demonstrated the mode-selective bond dissociation and resonant enhancement of photodesorption of hydrogen from Si–H using infrared laser excitation. For surface adsorbed species such as H on Si, the orientation of reagent molecules becomes important. To achieve the mode selectivity as well as the stereodynamic control of an adsorption process, the vibrationally excited molecules need to be oriented.[4–6]

Orientation and alignment imply confinement of the rotational axis in a given direction in space. For a molecular ensemble, it means a distribution of rotational states with well-defined quantum number M for the Z-component of the angular momentum J. The space fixed Z-axis may be the symmetry axis for a given experiment often coinciding either with the polarization direction of the laser field or the direction of beam propagation. Relative to this symmetry axis, the orientation is understood as a preferential direction of J regarded as a collection of single headed arrows (head versus tail). The alignment, on the other hand, implies a spatial distribution of J regarded as double headed arrows; in this case, the parallel and antiparallel orientations of J are indistinguishable. Following Zare,[7] the angular momentum polarization is best described by the orientation and alignment parameters as given below.

In the absence of Zeeman coherence, the ensemble averaged orientation parameter is

$$O = \frac{1}{\sqrt{J(J+1)}} \frac{\Sigma_{-J}^{J} \rho_{MM}^{JK} M}{\Sigma_{-J}^{J} \rho_{MM}^{JK}}, \tag{1}$$

and the alignment parameter is

$$A = \frac{1}{J(J+1)} \frac{\Sigma_{-J}^{J} \rho_{MM}^{JK} (3M^2 - J(J+1))}{\Sigma_{-J}^{J} \rho_{MM}^{JK}}. \tag{2}$$

Here, $\rho_{MM}^{JK} = \langle JKM|\rho|JKM\rangle \equiv$ population of the magnetic sublevel M in JK rotational state.

In the absence of external fields, optical or static, $\rho_{MM} \propto n_{JK}/(2J+1)$, and the molecules are isotropically distributed over the $2J+1$ magnetic sublevels. In this case, the summations in Eqs. (1) and (2) vanish, indicating no net orientation or alignment of molecular ensemble. Once this isotropy is broken by creating nonuniform population of the magnetic sublevels using optical excitation, molecules are oriented. As depicted schematically in Figs. 1(a) and 1(b), the orientation dependent photoexcitation cross section can be used to create nonuniform population in the magnetic sublevels. It is clear from Eq. (1) that an asymmetric distribution of Zeeman population excited by a σ polarized light, as in Fig. 1(b), would be necessary to induce a net orientation of the molecular ensemble. While the double headed nature of linear polarization exclusively induce alignment by creating a nonuniform symmetric distribution of Zeeman population as in Fig. 1(b). Note that the angular momentum polarization described above is directly related to the alignment of the molecular axis. This paper focuses on a new idea of molecular alignment using coherent resonant vibrational excitation with narrow linewidth infrared pulses. Since the early work of Drullinger and Zare,[8] the orientation dependent absorption cross section has been utilized to align molecular axis using radiation fields with well-defined polarization.[9–12] However, we will show here that under strong pumping condition, the spatial anisotropy is destroyed severely, limiting the alignment in an excited vibrational state.

[a)]Present address: Infrasign LLC, Palo Alto, CA 94306. Electronic mail: nandini@infrasign.com.

Among other optical techniques, we should note the work of Stapelfeldt and Seideman[13–15] on the adiabatic alignment of diatomic molecules using intense ultrashort pulses ($\sim$3 ns, peak intensity of $\sim$TW/cm^2). They also used intense picosecond and femtosecond pulses to impulsively excite and align rotational wave packets. Other groups achieved M state selection by applying a high intensity laser field to induce ac Stark shift to lift the degeneracy of the magnetic substates.[16,17] Combination of a strong dc Stark field ($\sim$10 kV/cm) and optical pumping has been used to demonstrate steric effect in the bimolecular reaction of HF with Li.[5]

More recently, rotationally cooled polar molecules have been aligned by spatially dispersing them with a strong inhomogeneous static field, followed by an adiabatic alignment with a high intensity (TW/cm^2) nanosecond laser.[18] Stimulated Raman scattering is very useful for orienting nonpolar symmetric molecules and is used with intense pulses to obtain optical alignment.[19] Recently, efficient M state selection of rotationally cooled H_2 and HD molecules is demonstrated using stimulated Raman pumping with a combination of 532nm Nd^{3+}:YAG (YAG denotes yttrium aluminum garnet) and a tunable pulsed dye laser.[20] M state selection has been theoretically predicted in chirped adiabatic Raman passage,[21] which exploits the orientation dependent Raman coupling and ΔM selection rule to align molecules in the high vibration levels. In most of these experiments, fairly intense electric fields (dc or optical) are required to achieve molecular alignment. In some of these experiments to achieve the field-free alignment, the intense electric fields associated with ultrashort pulses might trigger unwanted multiphoton ionization and dissociation of the reagent molecules.

This paper describes a different approach of field-free molecular alignment using coherent resonant interaction with narrow bandwidth single mode low power ($\leq$1 W) infrared laser sources [quantum cascade laser (QCL)]. The orientation dependent Rabi frequency associated with a two-level degenerate system of rovibrational transition is exploited for the M state selection. It is shown that, at least for small size molecules (NO_2, SO_2, CH_4, CH_3F, and NH_3), significant alignment in a single vibrational rotational excited state can be realized for the mode-selective stereodynamic control of chemical reaction. We must note the significant scope of this approach addressing a single rotational vibrational quantum state as opposed to the impulsive excitation addressing a group of rotational states (or wave packets) with intense femtosecond pulses.[13–15] We have pointed out in the beginning that it is difficult to populate and align molecules in an excited vibrational state because saturation under strong resonant pumping tends to destroy the orientation anisotropy. Although optically pumped molecular alignment in vibrational excited states has been considered for the purpose of steric control of a chemical reaction,[22] the effect of saturation on molecular alignment has not been examined. Our objective here is to address the problem of molecular orientation under strong optical pumping and explore the potential of coherent transient versus steady state excitation with ideal pulse shapes and energy to efficiently transfer and align the population in higher vibrational states.

Here, we should point out that the fast intra- and intermolecular energy redistributions shorten the lifetime of a coherently prepared molecular eigenstate. The optical energy deposited in a specific mode quickly leaks out into all other modes, leading to thermal equilibration or heating of the entire molecule. The detailed dynamics (pathways) and time frame of energy dissipation depend on the specific internal coordinate, the total number of degrees of freedom, their mutual interactions, and the energy deficits. For small size molecules considered here, the energy redistribution is caused mainly by the intermolecular collisions and, in general, the rate of $V \rightarrow V$ vibrational relaxation is faster than the $V \rightarrow T,R$ (vibration $\rightarrow$ translation, rotation). Extensive works of Flynn and co-workers[23–25] show that the intermode energy transfer in small polyatomic molecules can be slow enough to increase the temperature of a specific mode, enhancing the feasibility of mode-selective chemistry. For example, in SO_2 the relaxation of the stretching modes (ν_1 and ν_3) would require $\sim$135 collisions, the stretching modes of CH_3F would require $\sim$100 collisions, etc. These studies suggest that at low pressures ($<$1 Torr), the energy can be confined in a specific mode (the stretching mode of SO_2 or CH_3F) for sufficiently long time ($\sim$several microseconds) to initiate a mode-selective chemical reaction. The range of the gas pressures considered here is well within the range of real life deposition chambers. While the limited number of degrees of freedom in our examples reduces the energy relaxation rates of a specific mode, it does not point to a superficial idea, as in many chemical depositions we are concerned with surface reactions involving small size polyatomic molecules such as NH_3 or SiH_4.

The other limiting factor for achieving maximum alignment is the depolarization due to hyperfine interaction of J with the nuclear spin I. The M sublevels are mixed when J and I are strongly coupled, generating the hyperfine states with definite value of the total angular momentum F. However, we can expect the hyperfine depolarization rate to be small for fairly large values of the rotational angular momentum J since in this case J and F are nearly parallel. Moreover, using a narrow linewidth ($\sim$100 kHz) QCL, a single hyperfine level can be excited, increasing the lifetime of angular momentum polarization.[12,22,26]

This paper is organized as follows: First, we show that under coherent transient excitation, the alignment of vibrationally excited molecules becomes a function of the optical pulse area. Depending on the type of transition, with certain values of the pulse areas, a narrow group of magnetic substrates is selectively excited, which results in aligning the rotational angular momentum of the molecular ensemble. We compare the transient versus steady state excitation and show that under steady state excitation the alignment diminishes as the excitation saturates with stronger pump intensity. To describe the angular momentum distribution in the excited state, we calculate the alignment parameter for a P-type transition and show that for a pulse area of $\sim 2\pi$, significant alignment can be realized for molecules with arbitrarily large rotational angular momentum. Next, we introduce the idea of transferring the "2π pulse induced" optical alignment to a higher vibrational level using combined P- and Q-type step-

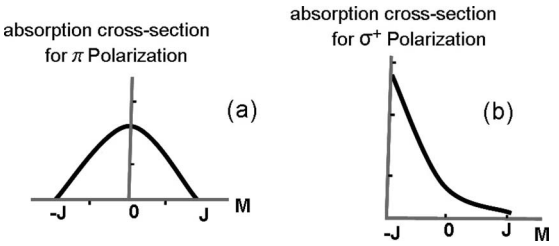

FIG. 1. Angular momentum polarization by selective photoexcitation. (a) Linearly polarized pump, Z-axis along the direction of polarization. (b) Circularly polarized pump, Z-axis along the propagation direction.

wise coherent excitations. The pulse areas and time delays between the P- and Q-type sequential transitions are adjusted to optimize the population transfer and alignment of a two-photon eigenstate. Finally, we discuss a polarization spectroscopy experiment for the real time probing of coherently aligned molecular states and their relaxation dynamics.

II. MOLECULAR ALIGNMENT UNDER COHERENT AND STEADY STATE EXCITATION

Our model system consists of the ground and excited rovibrational levels resonantly coupled to a π polarized electromagnetic field of a midwave infrared (MWIR) laser. Each rovibrational level is $(2J+1)$-fold degenerate over the projection of the rotational angular momentum J. In the case of linearly or circularly polarized radiation, the degenerate multilevel system decomposes into a set of independent two-level subsystems, which can be described by the Bloch equations. Under coherent excitation, a molecule interacts with a strong pump for a time period t less than the collision time t_c, and the population of the Zeeman sublevels is given by the analytic solutions of the optical Bloch equations. Using $\Delta M=0$ selection rule for a π polarized optical field and assuming zero detuning for simplicity, the population of the M sublevel in the excited manifold,

$$\rho_M = \tfrac{1}{2}[1 - \cos\Theta_M]. \tag{3}$$

The orientation dependent pulse area is

$$\Theta_M = \int \Omega_M dt, \tag{4}$$

where $\Omega_M=\mu_M E/\hbar$ is the Rabi frequency and μ_M is the component of the transition dipole moment parallel to the electric field E of the linearly polarized MWIR laser. μ_M is determined by the appropriate Clebsch–Gordan coefficients. For a P-type parallel transition,[27]

$$\mu_M = \mu\sqrt{A_{JK}}\sqrt{J^2 - M^2}, \tag{5}$$

where μ is the vibrational part of the transition dipole moment and

$$A_{JK} = \frac{J^2 - K^2}{J^2(2J-1)(2J+1)}. \tag{6}$$

The nonlinear dependence of the Zeeman population, ρ_M, on the pulse area Θ_M is exploited to create the anisotropic angular momentum distribution in the excited vibrational level

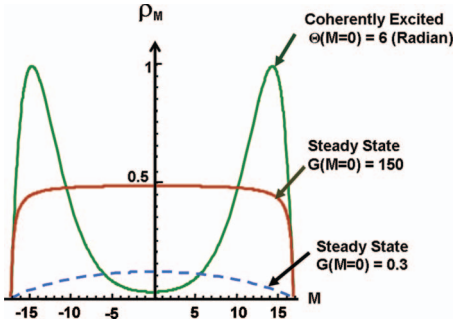

FIG. 2. Excited state population distribution among the Zeeman sublevels for steady state and coherent excitation with linearly polarized light. The angular momentum quantization Z-axis is oriented along the direction of the optical field.

of the molecule. The pulse area Θ_M is adjusted for optimum alignment.

The coherently excited population ρ_M in Eq. (3) should be compared to the following steady state expression of the excited state Zeeman population:

$$\rho_M^S = \frac{1}{2}\frac{G_M}{1+G_M}, \tag{7}$$

where ρ_M^S is found from the solutions of the rate equations describing the two-level subsystems under steady state excitation with long pulses (interaction time $t>t_c$). In this case, the orientation dependent saturation parameter G_M is used for the M state selection. The saturation parameter[27] $G_M = G_{JK}(J^2-M^2)$ with,

$$G_{JK} = \frac{2|\mu|^2 A_{JK}}{c\varepsilon_0 h^2\Gamma^2} I_P, \tag{8}$$

where Γ is the collisional damping rate and I_P is the intensity of MWIR laser.

Figure 2 shows the marked difference in the anisotropic distribution of the coherently excited and steady state population for different values of the saturation parameter G and pulse area Θ for a rotational state with $J=17$. The choice of the rotational quantum number is completely random and the results remain valid for arbitrary value of the rotational angular momentum J. Both the pulse area and the saturation parameter refer to the $M=0$ state. It should be noted that under steady state excitation, the anisotropy is drastically reduced due to saturation.

A. Alignment under steady state optical pumping

The alignment of a vibrationally excited molecular ensemble is defined by the alignment parameter A described earlier in Eq. (2). The alignment parameter is evaluated numerically for both steady state and coherently excited ensembles using appropriate density matrix elements ρ_M^J defined through Eqs. (3)–(8). Figure 3(a) shows the result of a numerical calculation of A under steady state excitation as a function of the saturation parameter G defined for the $M=0$ state for $J=17$. The saturation parameter G is proportional to the pump laser intensity. We have also plotted the fraction of the total population excited to the upper vibrational level. Figure 3(a) shows that maximum alignment is obtained in

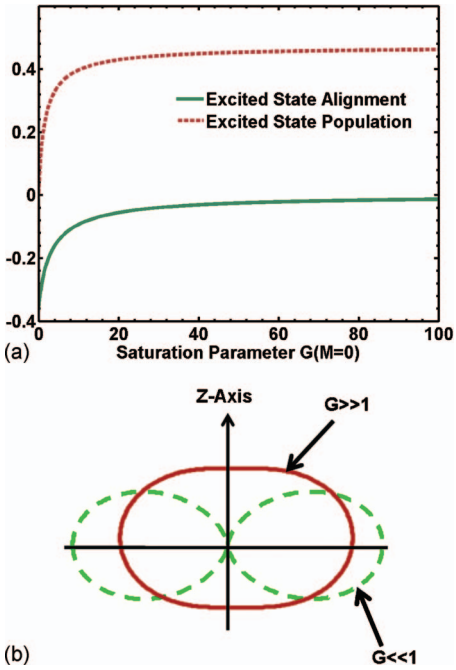

FIG. 3. (a) Excited state population and alignment vs saturation parameter G under steady state optical pumping. (b) Two-dimensional polar plot of excited state angular momentum distribution in the presence of low ($G \ll 1$) and high saturation ($G \gg 1$) under steady state optical pumping. The Z-axis is oriented along the polarization direction of the optical field.

the limit of small saturation or negligible excitation. With stronger laser intensity, the alignment is lost due to saturation.

For sufficiently large J (classical limit), the distribution of the angular momentum is defined by[12]

$$P_J(\theta) \cong \frac{1}{4\pi}\left[1 + \frac{5}{2}AP_2(\cos\theta)\right], \tag{9}$$

where θ is the angle between J- and the Z-axes aligned along the polarization direction of the optical field. $P_2(\cos\theta)$ is the second order Legendre polynomial and A is the alignment parameter. Following Eqs. (2) and (9), we must note that in the case of complete alignment parallel to the optical field ($M = \pm J$) $A \to 2$, giving a $\cos^2(\theta)$ distribution. Similarly, for a perfect alignment perpendicular to the optical field ($M=0$) $A \to -1$, giving a $\sin^2(\theta)$ distribution. Figure 3(b) is a polar plot for the angular momentum distribution function $P_J(\theta)$ in the limit of small and large pump intensities under steady state excitation. Figure 3(b) clearly shows that we lose molecular alignment under strong optical pumping.

B. Alignment under coherent excitation

Using the coherently excited density matrix ρ_M of Eq. (3) for a P-type parallel transition, we calculate the alignment parameter A [defined in Eq. (2)] as a function of optical pulse area Θ_0. Figure 4(a) shows the result of a numerical calculation for $J=17$. We have also plotted the fraction of the total population excited to the upper vibrational level at the end of the excitation pulse. Figure 4(a) shows that corresponding to the maximum alignment of $A \sim 1$ for a pulse area of $\sim 2.1\pi$, nearly 30% of the ground state molecules are

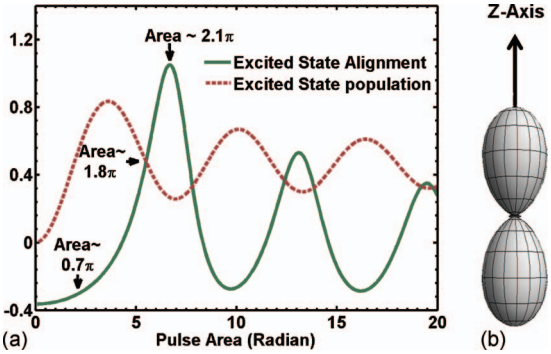

FIG. 4. (a) Excited state population and alignment vs optical pulse area under coherent resonant rovibrational excitation with linearly polarized light. (b) Angular momentum distribution of coherently excited molecules with 2π pulse area, Z-axis refers to the polarization direction of the optical field.

transferred to the excited level. As shown in Fig. 4(a), after a few oscillations, the alignment becomes more isotropic as more Zeeman levels get populated with increasing pulse area.

It can be shown that the pulse area for the maximum alignment in a P-type transition lie close to (within a few percent) $\sim 2\pi$ for all rotational levels $J > 5$. Figure 4(b) shows the three-dimensional polar plot of the angular momentum distribution corresponding to the maximum alignment for the 2π pulse area. Once the molecules are aligned in the first excited state, the population can be efficiently transferred to higher vibrational levels using stepwise coherent excitation with appropriate pulse area. In Sec. III, we describe a stepwise two-photon excitation and alignment in a higher vibrational level.

III. ALIGNMENT IN A COHERENTLY EXCITED TWO-PHOTON VIBRATIONAL LEVEL

For a P-type transition, a 2π pulse aligns the rotational angular momentum along the Z-axis by selectively pumping the magnetic sublevels with large values of M. Since a Q-type transition preferentially couples the large M states, intuitively we may expect to carry this alignment to the next higher vibrational level ($\nu=2$) using a proper combination of P- and Q-type sequential excitations. Note that the selection rules for the parallel and perpendicular bands (except for $K=0$ parallel band) of a symmetric top molecule will allow the coupling of P and Q transitions for the resonant excitation of a vibrational overtone.[28] In the following, we calculate the alignment parameter in the two-photon vibrational level induced by stepwise coherent excitation. We assume a P-type resonant transition connecting the ground and the first vibrational excited level ($1 \to 2$), followed by a Q-type transition between the intermediate and the two-photon excited level ($2 \to 3$). We also assume that the excitation pulses are linearly polarized and are separated in time. At reasonably low gas pressure (<1 Torr) with single mode cw lasers, the experiment can be realized by controlling the exposure times using Pockels cells. For a molecular beam, the pump lasers should be physically separated, their diameters adjusted for the optimum pulse area. For the linearly polarized optical

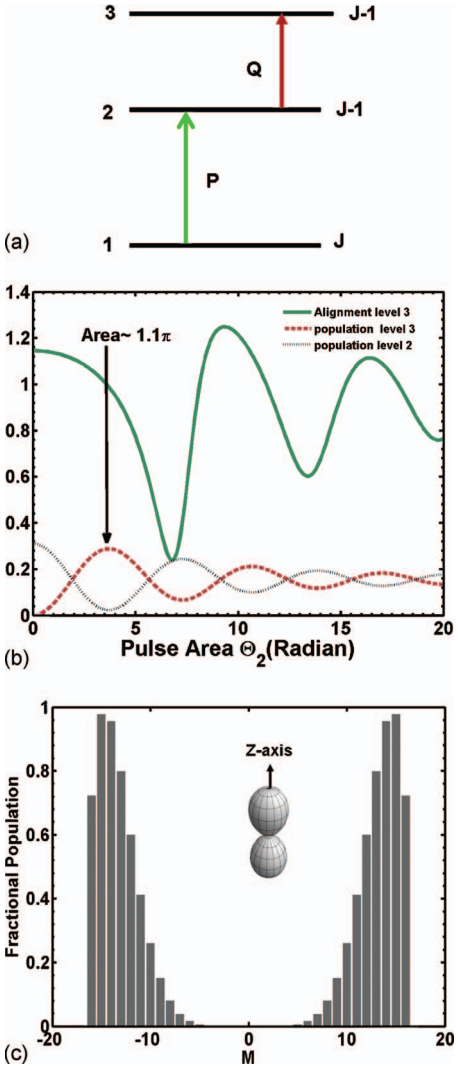

FIG. 5. (a) Level diagram for stepwise two-photon vibrational excitation with combined P-type $(1\rightarrow 2)$ and Q-type $(2\rightarrow 3)$ transitions. (b) Alignment parameter and excited state population as a function of the pulse area Θ_2 associated with the Q-type $(2\rightarrow 3)$ transition connecting the intermediate and the two-photon level. In the stepwise excitation, an optimum pulse area of $\Theta_1=2\pi$ is used for the P-type $1\rightarrow 2$ transition. (c) Zeeman population distribution in the two-photon excited level pumped by combined P-type (pulse area$=2\pi$) and Q-type (pulse area$=1.1\pi$) stepwise interactions. Polar plot of angular momentum distribution is shown in the inset. The space quantization Z-axis is directed along the linearly polarized optical field.

field $\Delta M=0$ selection rule is obeyed throughout the sequential excitation and the degenerate system is decoupled into independent three level subsystems with definite value of the magnetic quantum number M [see Fig. 5(a)]. We assume a collision free environment and the zero detuning for all transitions. At the end of the first excitation pulse, the population of the Mth magnetic sublevel of the intermediate rovibrational state $(\nu=1)$ is given by

$$\rho_{2M}^{J-1}=\tfrac{1}{2}[1-\cos\Theta_{M1}]. \tag{10}$$

In the absence of intramolecular vibrational relaxations, at the end of the second laser excitation, the Zeeman population in the two-photon rovibrational level $(\nu=2)$ is given by

$$\rho_{3M}^{J-1}=\rho_{2M}^{J-1}\times\tfrac{1}{2}[1-\cos\Theta_{M2}], \tag{11}$$

where Θ_{M1} and Θ_{M2} are the pulse areas associated with the P and Q transitions, respectively. Θ_{M1} for the P-type transition has been previously defined by Eqs. (4)–(6) in Sec. II.

The area for the Q-type transition

$$\Theta_{M2}=\int \mu_{23}^{M}\frac{E}{\hbar}dt,$$

where the transition dipole moment connecting the intermediate and the two-photon level, is given by

$$\mu_{23}^{M}=\mu_{23}\frac{MK}{J(J-1)}. \tag{12}$$

In the stepwise excitation, after a 2π pulse aligns the molecules in the intermediate level, the second laser coherently interacts with the aligned molecules and transfers them to the two-photon vibrational level $(\nu=2)$. Combing Eqs. (10)–(12) with Eqs. (4)–(6), we numerically calculate the alignment parameter [Eq. (2)] for the two-photon excited level. Figure 5(b) shows the alignment parameter as a function of the pulse area Θ_2 associated with the Q-type $(2\rightarrow 3)$ transition connecting the intermediate and the two-photon level. Optimum alignment and excitation is achieved with a P-type transition induced by a 2π pulse, followed by a Q-type transition with pulse area of $\sim 1.1\pi$. With this combination of pulse areas, the population of the two-photon level reaches $\sim 29\%$ of the ground state population, leaving $\sim 2\%$ population in the intermediate state. The optimum alignment parameter for the combined excitation is ~ 1. Figure 5(c) shows the Zeeman population distribution ρ_{3M}^{J-1} of the two-photon level. The corresponding angular momentum distribution of the two-photon excited molecules is shown in the inset.

The recent development of external cavity grating (ECG) tuned midinfrared (MIR) QCLs, producing hundreds of millwatts of power within a narrow spectral bandwidth $(\leq 0.0001\ \text{cm}^{-1})$,[27,29–31] has opened up the new possibility of addressing a single vibrational rotational quantum state using nonlinear optical interactions. A quick estimate shows that the ECG QCL meets the pulse area requirement of coherent excitation and alignment for a pressure of <1 Torr. Using a Gaussian beam diameter of ~ 3 mm and a transition dipole moment $\mu\sim 0.05$ D, the single photon Rabi frequency is estimated to be $\Omega\sim 0.8$ MHz. Therefore, the pulse area $\Theta(=2\pi\Omega t_p)$, corresponding to the maximum alignment, can be precisely adjusted by electro-optically switching the laser for an exposure time of a few microseconds. In Sec. IV, we describe an experiment to dynamically probe the coherently prepared molecular states using polarization spectroscopy with an ECG QCL.

IV. POLARIZATION SPECTROSCOPY EXPERIMENT TO PROBE MOLECULAR ALIGNMENT

Figure 6 shows the schematic of a polarization spectroscopy experiment to probe molecular alignment in real time as a function of optical pulse area, gas pressure, etc. In this experiment, a strong pump and a weak probe are counterpropagated through a long gas cell. When the MWIR laser is

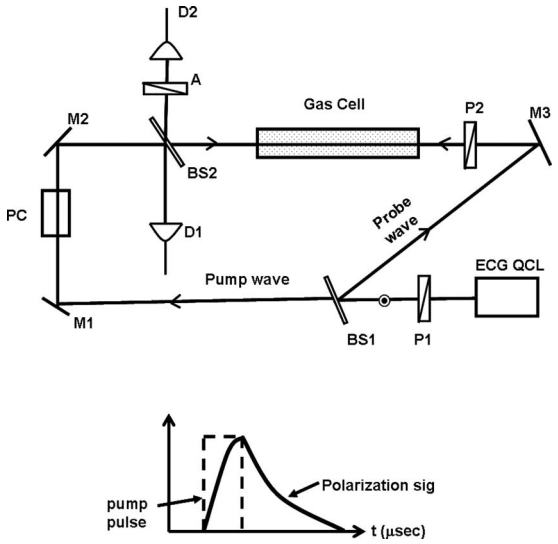

FIG. 6. Experimental setup for polarization spectroscopy. Mirrors: M1, M2, and M3; polarizers: P1 and P2; analyzer: A; Pockels cell: PC; beam splitters: BS1 and BS2; and HgCdTe detectors: D1 and D2.

tuned to the line center of a Doppler broadened rovibrational transition, the counterpropagating pump and probe interact with a common group of resonant molecules running perpendicular to the optical beam. Polarizer P1 defines the pump polarization along the Z-axis (the quantization axis), while polarizer P2 keeps the probe polarization at an angle of 45° relative to that of the pump. A is the analyzer that is nearly crossed with polarizer P2.

The pump induces transitions at different rates for sublevels with different magnetic quantum numbers (M); hence, the components of the probe polarization parallel and perpendicular to that of the pump will sense different saturation leading to different absorption and dispersion. Different propagation constants for the two polarization components will cause ellipticity and rotation of the plane of polarization of the probe electric field. The rotation of the probe polarization is detected with the analyzer at the output of the gas cell and is a direct measure of the pump-induced spatial anisotropy. To control the exposure time or the pulse area, the cw pump beam is switched on and off using an electro-optic switch (Pockels cell), while the weak probe continuously (adiabatically) watches the angular momentum polarization. In this experiment, we keep the laser beam diameter larger than the molecular mean free path, thus eliminating the effective decay of polarization due to fast transit across the pump beam. Under this condition, at a pressure of ~100 m Torr, a large molecular orientation can build up during a collision free excitation time of a few microseconds. After the strong pump orients the molecules for a few microseconds, it is suddenly switched off and the polarization signal decays with a characteristic relaxation time of a collision process. Both the rise and decay of the polarization signal can be recorded on a fast detector (nanosecond rise time). The peak of the polarization signal will be determined by the optical pulse area Θ (Θ=pump intensity $I_P \times t_P$). In the following, we establish the correspondence between the polarization signal and the alignment of the rotational angular momentum of the vibrationally excited molecules.

The detected light intensity behind the analyzer is given by[32]

$$I \cong I_0\left[\theta^2 + \theta\Delta\alpha\frac{L}{2} + \left(\frac{\Delta\alpha L}{4}\right)^2\right], \tag{13}$$

where θ is the uncrossing angle of the polarizer and the analyzer. $\Delta\alpha=\alpha_Z-\alpha_X$ is the induced anisotropy of probe absorption in presence of the pump. We assume that the probe intensity is only a few percent of the pump. In this approximation, the probe-induced change is negligible and the weak probe adiabatically senses the birefringence induced by the pump pulse. Assuming a P-type parallel transition in a symmetric top molecule and a π (or Z)-polarized pump beam, we can show that the absorption coefficient of the probe polarization parallel to the pump is given by

$$\alpha_Z = \alpha_0\frac{\Sigma_{-J}^{J}(\rho_M^J - \rho_M^{J-1})f_M^0}{\Sigma_{-J}^{J} f_M^0}, \tag{14}$$

where α_0 is the unsaturated (isotropic) absorption in the absence of the pump and

$$f_M^0 = J^2 - M^2, \tag{15}$$

ρ_M^J and ρ_M^{J-1} are the relative populations of the M sublevels in the ground $|v=0,JMK\rangle$ and excited $|v=1,J-1MK\rangle$ states, respectively. In the presence of a strong pump radiation, α_Z can differ significantly from α_0 and can even go to zero under strong saturation.

We can also derive the absorption coefficient for the X-polarized probe wave. The X-polarized probe wave resonantly couples the $|JM\rangle$ sublevel in the ground state with $|J-1M\pm1\rangle$ sublevels in the excited state. Therefore, the absorption of the X-polarized radiation is influenced by the relative population of the $|JM\rangle$ and $|J-1M\pm1\rangle$ sublevels. The absorption coefficient for the probe polarization perpendicular to the pump is given by

$$\alpha_X = \alpha_0\frac{\Sigma_{-J}^{J}[f_M^+(\rho_M^J - \rho_{M+1}^{J-1}) + f_M^-(\rho_M^J - \rho_{M-1}^{J-1})]}{\Sigma_{-J}^{J}(f_M^+ + f_M^-)}, \tag{16}$$

where $f_M^+=(J-M)(J-M-1)$ and $f_M^-=(J+M)(J+M-1)$.

The Zeeman populations (ρ_M^J and ρ_M^{J-1}) of the ground and excited states are found from the solutions of the two-level equations under the action of a strong pump both in steady state and in coherent regime. For simplicity, we assume resonant interaction with zero detuning, which corresponds to the maximum polarization signal at the line center of a Doppler broadened transition.

A. Polarization signal under steady state excitation

In the case of steady state excitation, the density matrix elements are the solutions of the two-level rate equations [Eq. (7)]. Figure 7 shows the result of a numerical calculation of $\Delta\alpha=\alpha_Z-\alpha_X$ under steady state excitation as a function of the saturation parameter G. Figure 7 shows that the polarization signal ($\propto\Delta\alpha/\alpha$) decreases with pump laser intensity. Under steady state excitation, we have seen similar behavior for the alignment parameter [see Fig. 3(a)]. The anisotropy is destroyed with saturation.

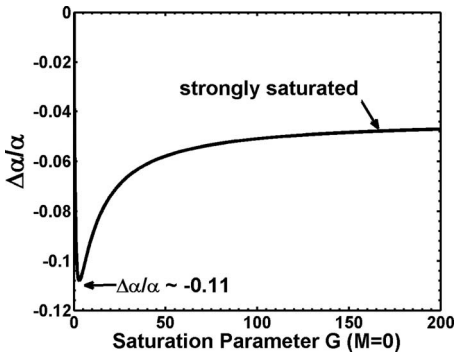

FIG. 7. Induced anisotropy $\Delta\alpha/\alpha$ vs saturation parameter G for steady state excitation with a linearly polarized pump laser.

B. Polarization signal under coherent excitation

For the coherently excited ensemble, we have calculated the anisotropy $\Delta\alpha/\alpha$ using density matrix elements found from the solution of the optical Bloch equations. These solutions are similar to that given in Eq. (3). The anisotropy and the alignment parameter are plotted in Fig. 8. Except for the small values of the pulse area of $<0.8\pi$, the polarization signal ($\propto\Delta\alpha/\alpha$) follows the molecular alignment maximizing for the pulse areas close to 2π. Thus, for pulse areas of $\geq 0.8\pi$, the molecular alignment can be mapped in real time using the time dependent polarization signal.

C. Relaxation dynamics of molecular alignment by polarization spectroscopy

As mentioned earlier, using the experimental setup shown in Fig. 6, we can directly measure the relaxation of molecular alignment from the decay rate of the polarization signal following an excitation pulse. The decay of the polarization signal can be described in the following way.

The decay of the Zeeman population in the excited rotational state $J-1$ (for a P-type transition) can be described as

$$\frac{d\rho_M^{J-1}}{dt} = -\gamma_M\rho_M^{J-1} + \sum_{M'\neq M}\frac{\gamma_M}{2(J-1)}\rho_{M'}^{J-1} - \gamma_{J-1}\rho_M^{J-1}, \quad (17)$$

where ρ_M^{J-1} is the population of the magnetic sublevel M. The decay rate due to the mixing of Zeeman sublevels (pure disorientation of J) is defined by γ_M and is assumed to be the same for all the sublevels for a given J. γ_{J-1} is the decay rate of the excited state due to inelastic collisions. The set of

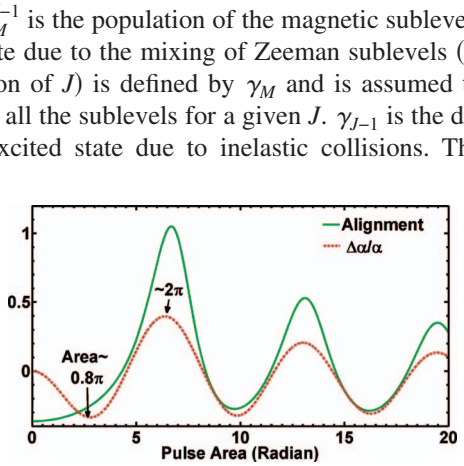

FIG. 8. Induced anisotropy $\Delta\alpha/\alpha$ and alignment parameter A vs optical pulse area under coherent resonant excitation with linearly polarized pump beam. The direct correlation between molecular alignment and $\Delta\alpha/\alpha$ suggests that polarization spectroscopy can be used as a real time probe for molecular alignment.

$2J-1$ coupled equations described by Eq. (17) can be solved to yield

$$\rho_M^{J-1}(t) = \left[\rho_M^{J-1}(0) - \frac{N_{J-1}(0)}{2J-1}\right]\exp\left[-\left(\frac{2J}{2J-1}\gamma_M + \gamma_{J-1}\right)t\right] + \frac{N_{J-1}(0)}{2J-1}\exp[-\gamma_{J-1}t], \quad (18)$$

where $N_{J-1}(0)$ is the total excited state population just when the pump is switched off.

The polarization signal is affected only by the M-dependent anisotropic term involving the Zeeman population $\rho_M^{J-1}(0)$ at the switching off time $t=0$. Following Eq. (18), it can be shown that, for fairly large value of the rotational quantum number J, the polarization signal decays as: $I=I(0)\exp[-(\gamma_M+\gamma_{J-1})t$.

If γ_M is significantly larger than the inelastic relaxation rate γ_{J-1}, for example, in the presence of strong hyperfine coupling with the nuclear spin, the decay of the polarization signal will directly measure the rate of hyperfine depolarization. Thus, the polarization spectroscopy provides an elegant and complete characterization of molecular alignment in rotational vibrational excited state. Similar polarization spectroscopy experiment using nonlinear optical Kerr effect was implemented to characterize the alignment of a rotational wave packet generated by impulsive excitation of high intensity femtosecond pulses.[33]

V. CONCLUSION

We have presented a new approach to align molecules in an excited vibrational level using coherent resonant excitation. The orientation dependent Rabi frequency associated with a two-level degenerate system of rovibrational transition is exploited for the M state selection. For the P-branch of a symmetric top molecule, a resonant MIR pulse of area $\approx 2\pi$ selectively populates the weakly coupled Zeeman levels and aligns the rotational axis along the polarization of the optical field. It is shown that under steady state excitation (pulse duration longer than the collisional relaxation time), the molecular alignment is destroyed due to saturation. Under coherent excitation with 2π pulse area, appreciable positive alignment ($A\approx 1$) is achieved with $\sim 30\%$ net excitation of the ground state population. The alignment shows the same functional dependence on the pulse area and maximizes at $\approx 2\pi$ for all rotational levels $J>5$. Due to the weak radiative decay rates of the vibrational levels in the ground electronic surface, the laser induced florescence technique[8] cannot be used to measure the anisotropic distribution of the angular momentum. Instead, here we design a polarization spectroscopy experiment to measure the molecular orientation. Our calculation shows that the signal in polarization spectroscopy is related to the alignment parameter and could be used as a real time probe for the optical alignment. In addition, using polarization spectroscopy the relaxation rates of molecular alignment due to collision and hyperfine depolarization can be measured from the decay of the polarization signal following a pulsed excitation.

Optical alignment in a higher vibrational level is accomplished using combined P- and Q-type stepwise coherent excitations. Optimum alignment in the two-photon excited level is achieved by a combination of P-type transition with a 2π pulse, followed by a Q-type transition with a π pulse. Our study has shown that the optimum alignment and population transfer in a combined P- and Q-type stepwise excitations are comparable to that obtained with two-photon adiabatic rapid passage (ARP). The two-photon excitation using ARP, however, requires much higher pulse intensity compared to the presently described stepwise coherent resonant process. The low power (<1 W) requirement for the coherent resonant excitation is particularly attractive for the application of tunable ECG QCLs to a variety of molecular reactions. Optical pulses from an external cavity QCL can be tailored toward the ideal pulse shape (area) to reach the maximum alignment for a given rotational vibrational eigenstate. The coherent alignment of molecules in a well-defined rovibrational state will open up new possibilities for characterizing gas surface reactions, where the interaction potential is a sensitive function of the molecular orientation relative to the surface normal or a crystal axis.[4,34]

ACKNOWLEDGMENTS

We would like to thank Professor C. Kumar N. Patel and Professor Richard N. Zare for helpful discussions.

[1] Z. Kary and R. N. Zare, J. Chem. Phys. **68**, 3360 (1978).
[2] M. P. Schmid, P. Maroni, R. D. Beck, and T. R. Rizzo, J. Chem. Phys. **117**, 8603 (2002).
[3] Z. Liu, L. C. Feldman, N. H. Tolk, Z. Zhang, and P. I. Cohen, Science **312**, 1024 (2006); see also J. C. Tully, *ibid.* **312**, 1004 (2006).
[4] E. W. Kuipers, M. G. Tenner, A. W. Kleyn, and S. Stolte, Phys. Rev. Lett. **62**, 2152 (1989).
[5] H. J. Loesch and F. Stienkmeler, J. Chem. Phys. **100**, 740 (1994); **98**, 9570 (1993).
[6] C. T. Rettner and R. N. Zare, J. Chem. Phys. **77**, 2416 (1982); R. N. Zare, Science **279**, 1875 (1998).
[7] R. N. Zare, *Angular Momentum Understanding Spatial Aspects in Chemistry and Physics* (Wiley Interscience, New York, 1988).
[8] R. E. Drullinger and R. N. Zare, J. Chem. Phys. **51**, 5532 (1969).
[9] R. N. Zare, Ber. Bunsenges. Phys. Chem **86**, 422 (1982).
[10] C. H. Greene and R. N. Zare, J. Chem. Phys. **78**, 6741 (1983).
[11] U. Hefter, G. Ziegler, A. Mattheus, A. Fischer, and K. Bergmann, J. Chem. Phys. **85**, 286 (1986).
[12] A. J. Orr-Ewing and R. N. Zare, Annu. Rev. Phys. Chem. **45**, 315 (1994).
[13] H. Stapelfeldt and T. Seideman, Rev. Mod. Phys. **75**, 543 (2003).
[14] T. Seideman, J. Chem. Phys. **103**, 7887 (1995).
[15] H. Stapelfeldt, Phys. Scr., T **110**, 132 (2004).
[16] A. F. Linskens, N. Dam, J. Reuss, and B. Sartakov, J. Chem. Phys. **101**, 9384 (1994).
[17] R. Neuhauser and H. J. Neusser, J. Chem. Phys. **103**, 5362 (1995).
[18] L. Holmegaard, J. H. Nielsen, I. Nevo, H. Stapelfeldt, F. Filsinger, J. Kupper, and G. Meijer, Phys. Rev. Lett. **102**, 023001 (2009).
[19] Y. B. Band and P. S. Julienne, J. Chem. Phys. **96**, 3339 (1992).
[20] N. C. M. Bartlett, D. J. Miller, R. N. Zare, D. Sofikitis, T. P. Rakitzis, and A. J. Alexander, J. Chem. Phys. **129**, 084312 (2008).
[21] F. Legare, S. Chelkowski, and A. D. Bandrauk, Chem. Phys. Lett. **329**, 469 (2000).
[22] J. Zhang, C. W. Riehn, M. Dulligan, and C. Wittig, J. Chem. Phys. **104**, 7027 (1996).
[23] D. R. Siebert, F. R. Grabiner, and G. W. Flynn, J. Chem. Phys. **60**, 1564 (1974).
[24] E. Weitz and G. Flynn, Annu. Rev. Phys. Chem. **25**, 275 (1974), and references therein.
[25] G. W. Flynn, Acc. Chem. Res. **14**, 334 (1981).
[26] R. Altkorn, R. N. Zare, and C. H. Greene, Mol. Phys. **55**, 1 (1985).
[27] N. Mukherjee and C. K. N. Patel, Chem. Phys. Lett. **462**, 10 (2008).
[28] G. Herzberg, *Infrared and Raman Spectra of Polyatomic Molecules* (D. Van Nostrand, Princeton, NJ, 1945).
[29] N. Mukherjee, R. Go, and C. K. N. Patel, Appl. Phys. Lett. **92**, 111116 (2008).
[30] G. Wysocky, R. F. Curl, F. K. Tittel, R. Maulini, J. M. Bulliard, and J. Faist, Appl. Phys. B: Lasers Opt. **81**, 769 (2005).
[31] M. Pushkarsky, A. Tsekoun, I. G. Dunayevskiy, R. Go, and C. K. Patel, Proc. Natl. Acad. Sci. U.S.A. **103**, 10846 (2006).
[32] C. Wieman and T. W. Hansch, Phys. Rev. Lett. **36**, 1170 (1976).
[33] V. Renard, M. Renard, S. Guerin, Y. T. Pashayan, B. Lavorel, O. Faucher, and H. R. Jauslin, Phys. Rev. Lett. **90**, 153601 (2003).
[34] E. W. Kuipers, M. G. Tenner, A. W. Kleyn, and S. Stolte, Nature (London) **334**, 420 (1988).